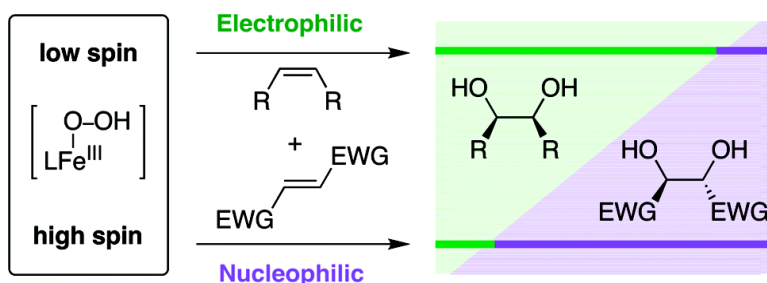


Iron-Catalyzed Olefin *cis*-Dihydroxylation by HO: Electrophilic versus Nucleophilic Mechanisms

Megumi Fujita, Miquel Costas, and Lawrence Que

J. Am. Chem. Soc., **2003**, 125 (33), 9912-9913 • DOI: 10.1021/ja029863d • Publication Date (Web): 26 July 2003

Downloaded from <http://pubs.acs.org> on March 29, 2009



More About This Article

Additional resources and features associated with this article are available within the HTML version:

- Supporting Information
- Links to the 8 articles that cite this article, as of the time of this article download
- Access to high resolution figures
- Links to articles and content related to this article
- Copyright permission to reproduce figures and/or text from this article

[View the Full Text HTML](#)

Iron-Catalyzed Olefin *cis*-Dihydroxylation by H₂O₂: Electrophilic versus Nucleophilic Mechanisms

Megumi Fujita, Miquel Costas, and Lawrence Que, Jr.*

Department of Chemistry and Center for Metals in Biocatalysis, University of Minnesota, Minneapolis, Minnesota 55455

Received December 20, 2002; E-mail: que@chem.umn.edu

The first examples of nonheme iron complexes to catalyze olefin *cis*-dihydroxylation by H₂O₂ have recently been reported.¹ Olefin epoxidation is observed as well, and the *cis*-diol/epoxide ratio can be tuned by the nature of the metal coordination environment.^{1a-c} In general, the catalysts have mononuclear iron(II) centers coordinated to tetradentate ligands that allow *cis* labile sites and convert to active Fe^{III} forms upon treatment with H₂O₂. On the basis of reaction behavior, these catalysts can be categorized into two classes. Class A catalysts form low-spin Fe^{III}-OOH intermediates and give rise to *cis*-diol products with one oxygen atom derived from H₂O₂ and the other from H₂O.^{1a,b} On the other hand, Class B catalysts afford high-spin Fe^{III}-OOH intermediates and give rise to *cis*-diol products with both oxygen atoms coming from a single molecule of H₂O₂.^{1a,2} On the basis of these observations, different spin-state-dependent mechanisms have been suggested for these two classes (Scheme 1). Compelling evidence has been obtained for the participation of an Fe^V(=O)OH oxidant for Class A catalysts, a notion supported by DFT calculations,³ but the nature of the Class B oxidant is less understood. To gain further insight into the mechanistic differences between class A and B catalysts, we have investigated the oxidation of electron-deficient olefins and found that the active intermediate(s) responsible for olefin oxidation are, respectively, electrophilic and nucleophilic in character.

Complexes [(TPA)Fe(OTf)₂] (**1**) and [(6-Me₃-TPA)Fe(OTf)₂] (**2**)⁴ have been selected as prototypical for classes A and B, respectively. In contrast to its oxidation of electron-rich olefins that affords both epoxide and *cis*-diol products, **1** catalyzes oxidation of electron-deficient olefins to afford only *cis*-diol products in good to excellent yield (turnover numbers of 6–9.5 from 10 equiv of H₂O₂) (Table 1). In fact, the oxidation of dimethyl fumarate to dimethyl *rac*-tartrate is essentially quantitative (entry 5), because 0.5 equiv/Fe of H₂O₂ is required to convert the iron(II) catalyst to its active iron(III) form.^{1a} For **2** as well, electron-deficient olefins are converted only to diols, but turnover numbers range from 4 to 7, consistent with its observed lower efficiency in oxidations of electron-rich olefins (Table 1).

Further experiments show that the respective oxidations of electron-deficient olefins by **1** and **2** follow the patterns previously established with electron-rich olefins.^{1b} In the conversion of dimethyl fumarate to dimethyl *rac*-tartrate, there is >99% retention of configuration for both catalysts. ¹⁸O-Labeling studies (Table S1) show that the diol from **1** incorporates one oxygen atom each from H₂O₂ and H₂O, while that from **2** derives both oxygen atoms from H₂O₂, strongly suggesting that the same oxidizing intermediate is involved in oxidation of both electron-rich and electron-deficient olefins for each catalyst (Scheme 1). In contrast, the *cis*-dihydroxylation of dimethyl maleate results in some epimerization, with RC values of 79% for **1** and 10% for **2** (entry 6, Table 1). Despite the loss in stereochemistry, ¹⁸O-labeling experiments show the same oxygen incorporation pattern as for the other olefins (Scheme 1,

Table 1. Olefin Oxidation Products^a

entry	olefin	1	2
		diol/epoxide ^b [%RC] ^c	diol/epoxide ^b [%RC] ^c
1	acrylonitrile	8.5(4)/–	7.3(7)/–
2	methacrylonitrile	7.0(12)/–	6.9(12)/–
3	<i>tert</i> -butyl acrylate	5.8(8)/–	6.2(6)/–
4	ethyl <i>trans</i> -crotonate	6.9(5)/– [>99]	4.5(1)/– [>99]
5	dimethyl fumarate	9.5(3)/– [>99]	5.2(4)/– [>99]
6	dimethyl maleate	7.8(4)/– [79]	4.2(3)/– [10]
7	<i>cis</i> -2-heptene ^{1b}	3.0(3)/1.9(1) [96]	4.1(4)/0.4(1) [93]
8	<i>cis</i> -cyclooctene ^{1b}	4.2(2)/3.4(1)	4.9(6)/0.7(2)
9	1-octene	6.1(3)/1.1(2)	4.7(9)/0.1(1)

^a Reaction conditions: An H₂O₂ solution (21 μ mol or 0.30 mL of a 70 mM solution in CH₃CN with ≥ 245 mM H₂O) was added via syringe pump over 22 min to a solution of olefin (1050 μ mol) and the catalyst (2.1 μ mol) in CH₃CN (2.7 mL) at 22–25 °C under air. ^b Yield expressed as turnover numbers (μ mol product/ μ mol catalyst) determined by GC analysis; average of 2–3 runs. ^c %RC: $100 \times (A - B)/(A + B)$ where A = yield of *cis*-diol with retention of configuration and B = yield of epimer.

Scheme 1

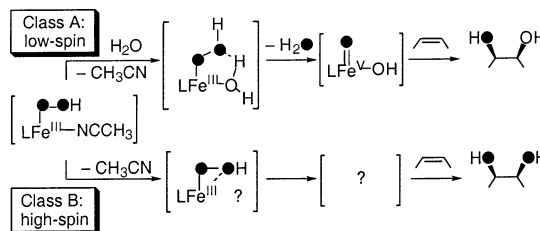


Table S1), indicating that O₂ does not play a role in these reactions. The observed loss of stereochemistry requires that the two C–O bonds of the diol product form in a stepwise mechanism for both catalysts.

Competition experiments reveal the most significant difference in the nature of the oxidants generated by **1** and **2**. Figure 1 shows the results of pairwise oxidations among four olefins: cyclooctene (two alkyl substituents), 1-octene (one alkyl substituent), *tert*-butyl acrylate (one electron-withdrawing group or EWG), and dimethyl fumarate (2 EWGs). These results demonstrate that **1** clearly prefers to oxidize the more electron-rich olefin, while **2** has the opposite preference. For example, between cyclooctene and *tert*-butyl acrylate, **1** favors cyclooctene oxidation by a factor of 4, while **2** favors *tert*-butyl acrylate oxidation by a factor of 4. The opposite preferences exhibited by **1** and **2** imply the formation of distinct oxidants. The reactivity of **1** is consistent with an electrophilic oxidant, presumably the Fe^V(=O)OH species implicated by earlier ¹⁸O-labeling results (Scheme 1). The contrasting behavior of **2**, on the other hand, suggests formation of a nucleophilic oxidant.

Thus far, there are two literature examples of nucleophilic substrate oxidations by high-spin iron(III) peroxo species. In case

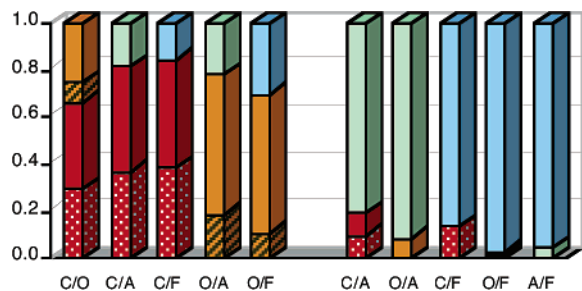
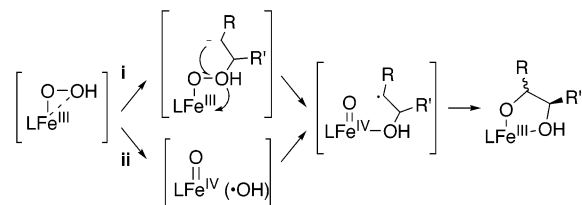


Figure 1. Competition experiments for the oxidation of olefin pairs by catalysts **1** (left) and **2** (right): C = cyclooctene (red), O = 1-octene (orange), A = *tert*-butyl acrylate (green), F = dimethyl fumarate (blue). Conditions as described under Table 1 except that 1050 μmol each of two olefins was used. Solid blocks represent the fraction of diol formed, while patterned blocks represent the fraction of epoxide formed.

Scheme 2. Proposed Mechanisms of *cis*-Dihydroxylation by a Nucleophilic Oxidant Generated from **2**/ H_2O_2



I, epoxidation of α,β -unsaturated ketones is initiated by nucleophilic attack of an (η^2 -peroxy)iron(III) porphyrin complex,⁵ followed by O–O bond heterolysis, analogous to the action of basic H_2O_2 . In case II, a high-spin $\text{Fe}^{\text{III}}-\eta^1\text{-OOH}$ intermediate is proposed to undergo O–O bond homolysis to generate a species that preferentially oxidizes dimethyl sulfoxide over dimethyl sulfide.⁶ To apply to **2**, these mechanisms must be adapted to account for the unprecedented formation of *cis*-diol and its high yield.

Scheme 2 shows two proposed mechanisms for *cis*-dihydroxylation by **2**. Mechanism **i** entails a nucleophilic attack by the coordinated peroxide on the olefin, like case I, but followed by reductive O–O bond homolysis. Mechanism **ii** involves initial O–O bond homolysis, like case II, to form a tightly associated $\text{Fe}^{\text{IV}}=\text{O}/\text{HO}\cdot$ pair, followed by nucleophilic attack of $\text{HO}\cdot$ on the substrate. (The nucleophilicity of $\text{HO}\cdot$ has been documented by Walling and El-Taliawi, who showed that $\text{HO}\cdot$ readily adds to α,β -unsaturated acids to form water addition products (but not diols).⁷) In both mechanisms, the available *cis* site on the iron center is recruited to facilitate formation of an $\text{Fe}^{\text{IV}}-2\text{-hydroxyalkyl}$ radical species. This species is the key to diol formation, as iron complexes of related pentadentate ligands do not catalyze *cis*-dihydroxylation.^{1,8} The subsequent collapse of this Fe^{IV} -radical species to diol is akin to the oxygen rebound step in iron-catalyzed alkane hydroxylations.⁹ The rate of oxygen rebound depends on the stability of the transient alkyl radical, thus affording a high RC value for *cis*-2-heptene and a lower value for dimethyl maleate due to the radical-stabilizing effect of the adjacent $-\text{COOMe}$ group.

In summary, we have found that **1** and **2**, respectively, generate oxidants with electrophilic and nucleophilic character in the catalysis

of olefin *cis*-dihydroxylation by H_2O_2 . This difference is likely related to the spin state of the $\text{Fe}^{\text{III}}-\text{OOH}$ intermediate generated in the course of catalysis. The electrophilicity of the oxidant derived from **1**/ H_2O_2 is consistent with the reactivity expected for the previously proposed high-valent $\text{Fe}^{\text{V}}(=\text{O})\text{OH}$ species derived from a low-spin $\text{Fe}^{\text{III}}-\text{OOH}$ intermediate.^{1a,b} Such a species may be viewed as related to the high-valent dioxometal species well known to carry out olefin *cis*-hydroxylation.¹⁰ The observed nucleophilicity of the oxidant generated from **2**/ H_2O_2 , on the other hand, has fewer precedents and requires the consideration of new mechanisms to rationalize the high conversion efficiency and stereoselectivity associated with the putative high-spin $\text{Fe}^{\text{III}}-\text{OOH}$ intermediate. This study thus establishes the mechanistic versatility of iron-peroxo species in olefin oxidation; it also lays the foundation for understanding the mechanism of Rieske dioxygenases,¹¹ enzymes involved in biodegradation that catalyze *cis*-dihydroxylation of arenes and olefins.

Acknowledgment. This work was supported by the National Institutes of Health (GM-33162) and the Petroleum Research Fund administered by the American Chemical Society (38602-AC). M.C. is grateful to Fundacio La Caixa for a postdoctoral fellowship that in part supported his stay at the University of Minnesota. We appreciate the thoughtful input of one reviewer in formulating mechanisms for Scheme 2.

Supporting Information Available: Table S1 listing results of ^{18}O -labeling experiments (PDF). This material is available free of charge via the Internet at <http://pubs.acs.org>.

References

- (1) (a) Chen, K.; Costas, M.; Que, L., Jr. *J. Chem. Soc., Dalton Trans.* **2002**, 672–679. (b) Chen, K.; Costas, M.; Kim, J.; Tipton, A. K.; Que, L., Jr. *J. Am. Chem. Soc.* **2002**, *124*, 3026–3035. (c) Costas, M.; Que, L. *Angew. Chem., Int. Ed.* **2002**, *41*, 2179–2181. (d) Costas, M.; Tipton, A. K.; Chen, K.; Jo, D.-H.; Que, L., Jr. *J. Am. Chem. Soc.* **2001**, *123*, 6722–6723. (e) Chen, K.; Que, L., Jr. *Angew. Chem., Int. Ed.* **1999**, *38*, 2227–2229.
- (2) Zang, Y.; Kim, J.; Dong, Y.; Wilkinson, E. C.; Appelman, E. H.; Que, L., Jr. *J. Am. Chem. Soc.* **1997**, *119*, 4197–4205.
- (3) Bassan, A.; Blomberg, M. R. A.; Siegbahn, P. E. M.; Que, L., Jr. *J. Am. Chem. Soc.* **2002**, *124*, 11056–11063.
- (4) TPA = tris(2-pyridylmethyl)amine; 6-Me₃-TPA = tris(6-methyl-2-pyridylmethyl)amine.
- (5) Wertz, D. L.; Valentine, J. S. *Struct. Bonding* **2000**, *97*, 38–60 and references therein.
- (6) Wada, A.; Ogo, S.; Nagatomo, S.; Kitagawa, T.; Watanabe, Y.; Jitsukawa, K.; Masuda, H. *Inorg. Chem.* **2002**, *41*, 616–618.
- (7) Walling, C.; El-Taliawi, G. M. *J. Am. Chem. Soc.* **1973**, *95*, 844–847.
- (8) Roelfes, G.; Lubben, M.; Hage, R.; Que, L., Jr.; Feringa, B. L. *Chem.-Eur. J.* **2000**, *6*, 2152–2159.
- (9) Groves, J. T. *J. Chem. Educ.* **1985**, *62*, 928–931.
- (10) (a) Johnson, R. A.; Sharpless, K. B. *Catalytic Asymmetric Synthesis*; VCH: New York, 1993; pp 227–271. (b) Schröder, M. *Chem. Rev.* **1980**, *80*, 187–213. (c) Shing, T. K. M.; Tam, E. K. W.; Tai, V. W.-F.; Chung, I. H. F.; Jiang, Q. *Chem.-Eur. J.* **1996**, *2*, 50–57.
- (11) (a) Que, L., Jr.; Ho, R. Y. N. *Chem. Rev.* **1996**, *96*, 2607–2624. (b) Kauppi, B.; Lee, K.; Carredano, E.; Parales, R. E.; Gibson, D. T.; Eklund, H.; Ramaswamy, S. *Structure* **1998**, *6*, 571–586. (c) Wolfe, M. D.; Parales, J. V.; Gibson, D. T.; Lipscomb, J. D. *J. Biol. Chem.* **2001**, *276*, 1945–1953. (d) Wolfe, M. D.; Lipscomb, J. D. *J. Biol. Chem.* **2003**, *278*, 829–835. (e) Karlsson, A.; Parales, J. V.; Parales, R. E.; Gibson, D. T.; Eklund, H.; Ramaswamy, S. *Science* **2003**, *299*, 1039–1042.

JA029863D